Asian Journal of Green Chemistry 3 (2019) 236-257

Asian Journal of Green Chemistry

Journal homepage: www.ajgreenchem.com

Original Research Article

Cationic dye (methyl violet) removal from aqueous solution by egg membrane in a batch biosorption process

Beniah O. Isiuku[a,*], Chigoziri Ugwueze Nwogu[b]

[a] *Department of Chemistry, Imo State University, Owerri, Nigeria*

[b] *Department of Chemistry, Faculty of Science, Imo State University, Owerri, Nigeria*

ARTICLE INFORMATION

Received: 28 August 2018
Received in revised: 9 October 2018
Accepted: 28 October 2018
Available online: 16 January 2019

DOI: 10.33945/SAMI/AJGC.2019.3.8

KEYWORDS

Batch biosorption
Egg membrane
Liquid film diffusion
Methyl violet
Modeling

ABSTRACT

Non-modified egg membrane was used to remove methyl violet from aqueous solution by batch biosorption at various experimental conditions. Isotherm, kinetic and thermodynamic as well as biosorption mechanism were investigated and discussed. Dye uptake increased with increase in initial dye concentration but decreased with increase in time. Maximum biosorpion capacity and optimum temperature were 161 mg/g and 45 °C respectively. Liquid film diffusion controlled the process which was endothermic, spontaneous and physisorptive. Egg membrane appears to be a novel natural membrane for removing cationic substances from aqueous solutions. It is environmentally friendly.

Corresponding author, email: obinnabisiuku@yahoo.com (B.O. Isiuku).
Tel: +2348 035731300.

Graphical Abstract

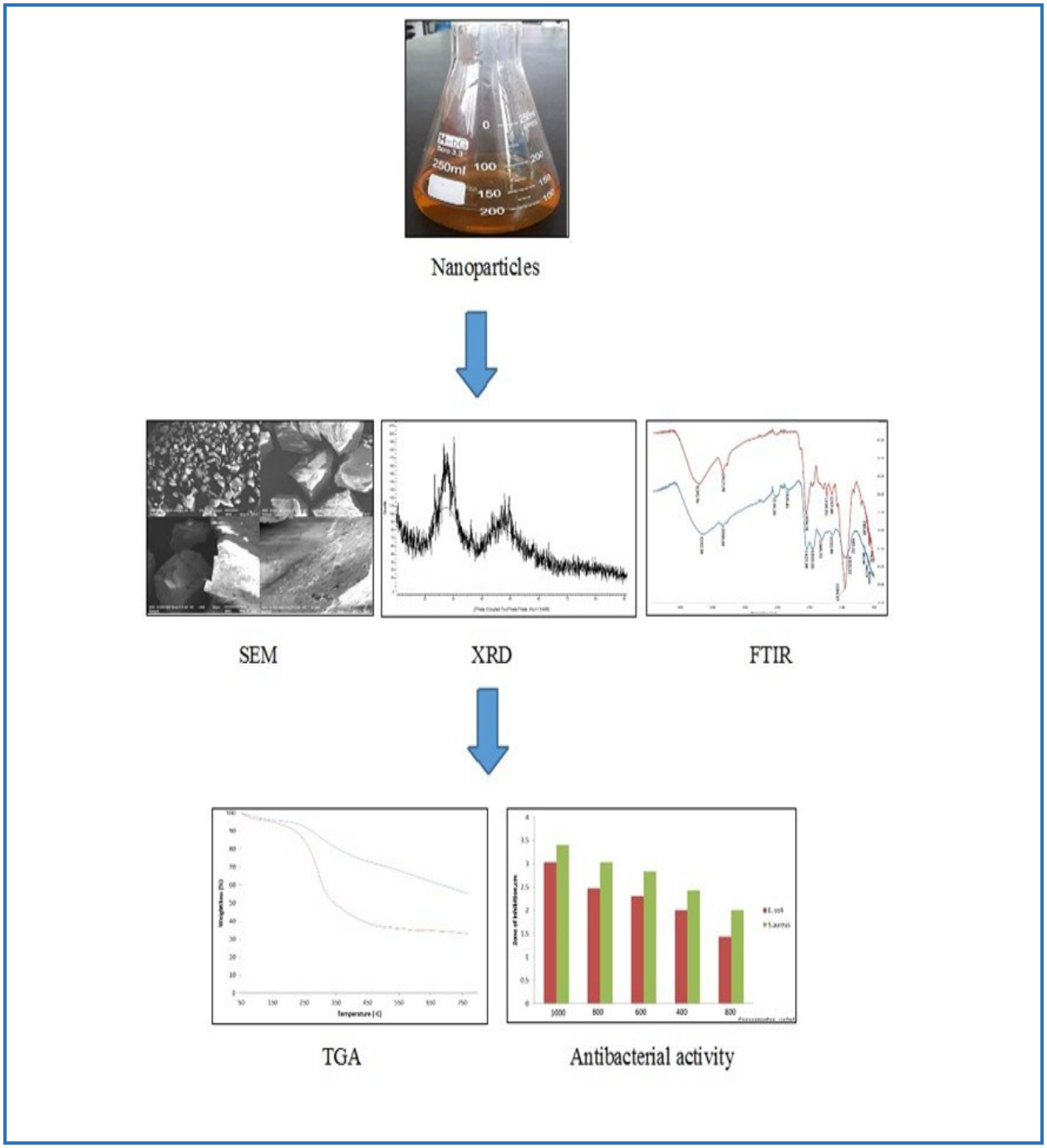

Introduction

There has been a growing public concern over the disposal of dye wastewater from textile and dyestuff industries into water bodies due to their toxicity and carcinogenicity [1]. The discharge of wastewater into water bodies which is aesthetically displeasing, hinders penetration of light needed

for photosynthesis in aquatic plants, damages the quality of the receiving water bodies and is detrimental to aquatic life [2].

Dyes are chemicals which impart color permanently on materials due to chemical bonding. They are ionic and aromatic organic compounds having delocalized electron systems. The color of a dye arises from the presence of a chromophore. A chromophore is a radical configuration made up of conjugated double bonds possessing delocalized electrons. The chromogen, which is an aromatic system contains benzene, naphthalene or anthracene rings which form a part of a chromophore–chromogen structure along with an auxochrome. The ionic moieties termed as auxochromes are responsible for a much stronger change of the maximum light absorption of the dye and provide a bonding affinity [3]. Methyl violet is broadly applied in paints, textiles, printing inks, bacteria classification and as a disinfectant [4, 5]. Inhalation of methyl violet may cause irritation to the respiratory tract. Its ingestion causes irritation to the gastrointestinal tract [6]. Methyl violet is difficult to degrade due to the presence of three phenyl groups, each bonded to a nitrogen atom which interacts with one or two methyl groups [7].

Many technologies have been developed for removing synthetic dyes from wastewater in order to control environmental pollution. They include membrane filtration processes, adsorption techniques, coagulation, advanced oxidation processes and ozonation [8]. Among the technologies, adsorption is superior to the other techniques in terms of cheapness, flexibility, simplicity of design, ease of operation and lack of sensitivity to toxicants [9, 10].

Adsorption is a process that takes place at the surface as a result of the sticking of the particles (Atoms, ions or molecules) of one substance (Adsorbate) to the surface of the other (Adsorbent) [1]. Biosorption is the adherence of an adsorbate on the surface of the adsorbent where the adsorbent is a natural material of biological origin whether living or denatured [11]. *Hen* egg membrane has good biosorption characteristics. It comprises from polysaccharide fibres and collagen which contain hydroxyl, amine and sulphonic functional groups which bind the biosorbate particles [12]. Hen egg membrane has been found useful in supporting immobilisation of enzymes [13]. *Pramanpol* and *Nitaya pat*, [13] removed C.I. reactive Yellow 205 with eggshell containing the membrane and non-membrane. Their results showed that the presence of the membrane created an increase in biosorption capacity 10-27 folds. *Hassan* and *Salih*, [12] used eggshell containing the membrane to effectively remove methylene blue, a cationic dye, from aqueous solution.

This work investigated the effectiveness of hen egg membrane in the removal of methyl violet from aqueous solution by a batch biosorption process. The effects of initial dye pH, initial solution concentration C_o, temperature and adsorbent dosage were investigated.

Experimental

Biosorbate

The methyl violet (M/s Deverson, India) used in this work was purchased at Onitsha, Nigeria and used with no further treatment. (Scheme 1) shows the structure. The stock solution was prepared by dissolving 1 g dye per litre solution in a 1 L volumetric flask using deionized water.

Preparation of the biosorbent

The eggshell waste was obtained from restaurants at Imo State University, Owerri, Nigeria. The waste was washed thoroughly with hot distilled water to remove dirt. It was packed in a stainless steel vessel containing deionized water and boiled for 30 min. After cooling, while still soaked in water, the membrane was peeled off. The peels biomass was dried at 105 °C for 24 h. After cooling the biomass was ground and sieved to obtain 0.42-0.841 mm particles. The biomass was packed in a plastic container.

Characterization of the biosorbent

Infrared spectrophotometric analysis was run with a sample of the hen egg membrane with UV/Visible spectrophotometer (FT-IR-8400S, M/s Shimadzu, Japan). Proximate analysis of the biosorbent was carried out using the method of the Association of Official Analytical Chemists [14]. The surface structure of the egg membrane was examined with a scanning electron microscope (SEM model Phenom Prox, M/s Phenom world, Netherlands).

Batch biosorption process

Batch biosorption of methyl violet from aqueous solution was carried out by agitating 0.01 g portions of the hen egg membrane with 25 mL portions of different C_o values in 50 mL volumetric flasks. This was done by setting the samples flasks in a water bath shaker and, then, agitating it for 6 h at 30 °C and a speed of 150 rpm. A sample was collected each hour, filtered, and, then, the filtrate was analyzed using UV-Visible spectrophotometer (Shimadzu, model 752, M/s Shimadzu, China) at a wavelength of 640 nm λ_{max}.

Effect of initial pH

Akinola and Umar [15] method was applied. Fifty mL portions of methyl violet solution, C_o 25 mg/L were measured into six 100 mL conical flasks. The portions of the solution in the various flasks were adjusted to pH 6-10 with 1M NaOH solution. 0.02 g portions of the membrane which were introduced into the flasks which were then agitated in a water bath shaker at 150 rpm speed at 30 °C

for 3 h. Sample solutions were filtered into sample tubes for analysis. The analysis was done using a UV/Vis spectrophotometer.

Effect of initial concentration and contact time

The method of *Rocha* et al., [16] was used. Fifty mL portions of the dye solution were measured into 100 mL conical flasks. 0.02 g hen egg membrane was added into each flask. The flasks were agitated at 150 rpm in a water bath shaker at 30 °C. Three flasks of C_o 25, 50 and 100 mg/L were removed at 30 min intervals for a total agitation time of 7 h. Clear solutions were collected from the flasks with syringes into sample tubes. Solution samples were analyzed with UV/Vis spectrophotometer at 640 nm $\lambda_{max.}$

The biosorption capacity q_t at time t (min) and equilibrium q_e (mg/g) were calculated [11] using Eqs. 1 and 2:

$$q_t = \frac{(C_o - C_t)v}{1000\,m} \quad (1)$$

$$q_e = \frac{(C_o - C_e)v}{1000\,m} \quad (2)$$

Where, C_o, C_t, C_e, (mg/L), v (mL), and m (g) are dye concentrations at time t = 0, t = t and at equilibrium, the volume of solution and the dry mass of the egg membrane respectively.

The total percentage removal, R (%), of the dye by the membrane (Biosorbent efficiency) was calculated using Eq. 3:

$$R(\%) = \frac{(C_o - C_e)100}{C_o} \quad (3)$$

The biosorption capacity and R (%) are related according to Eq. 4:

$$q_e = \frac{R\,C_o\,V}{10^5\,m} \quad (4)$$

Effect of biosorbent dosage

Fifty millilitre portions of the dye solution, C_o 25 mg/L and pH 8, were introduced into five 100 mL conical flasks. The masses of the hen egg membrane added to the flask varied from 0.02-0.32 g. The flasks were stoppered and agitated in a water bath shaker at 30 °C and 150 rpm speed for 5 h.

Clear solutions were taken from the flasks using syringes into sample tubes for analysis using UV/Vis spectrophotometer at 640 nm λ_{max}.

Effect of temperature

Fifty mL portions of the dye solution of C_o 25, 50 and 100 mg/L at pH 8, were introduced into three 100 mL conical flasks. 0.02 g of hen egg membrane was added into each flask. The flasks were stoppered and agitated in a water bath shaker at 30 °C and speed 150 rpm for 3 h. The suspensions were filtered into sample tubes and analyzed with the UV/Vis spectrophotometer at 640 nm λ_{max}. The process was repeated at 45 and 60 °C respectively.

Results and discussion

Analysis of the biosorbent

Fourier transform infrared spectrophotomeric analysis and proximate analysis were carried out on the egg membrane. (Table 1) shows the protein, carbohydrate, fibre, and lipid contents of the biomass. (Figure 1) shows the infrared spectrum of the biosorbent. The infra-red peaks at 2341.66, 2843.17, 3036.06, 3255.95, and 3618.58 cm^{-1} indicate the presence of N–H and O–H functional groups, while 1238.34, 1408.08, 1519.96, and 1658.84 cm^{-1} show the presence of –CO functional group. The N–H and –CO functional groups exist in protein and protein fibres. Carbohydrates furnish O–H, and esters (Lipids) contain –CO and C–O functional groups [17–19]. (Figures 2**a** and **b**) show the scanning electron micrographs of egg membrane which has a mesh structure with pores of different sizes. The combination of the functional groups and pores are responsible for the biosorption on the biomass.

Effect of initial concentration and contact time

The effect of contacting 0.01 g portions of hen egg membrane with 25 mL portions of methyl violet at pH 8 and 30 °C is portrayed in Figure 3. It was observed that biosorption capacity q_e increased with increase in C_o but decreased with increase in time. The highest biosorption capacity values of 55.675, 94.525 and 161.925 mg/g were obtained for C_o 25, 50 and 100 mg/L respectively with in 30 min of contact while the least values of 32.95, 64 and 122.15 mg/g respectively were at 420 min. The increase in q_e with increase in C_o might be related to the increase in the driving force needed to overcome the resistance of methyl violet ions migration from the dye solution to the biosorbent surface [12]. At higher dye concentrations, the active sites of the hen egg membrane were surrounded by much more methyl violet ions leading to enhanced biosorption [20]. Hen egg membrane consists of a network of fibrous proteins whose surface has positively charged sites produced by the side

chains of the amino acids, arginine and lysine [13–21]. Due to the faintly alkaline pH (pH 8) [13] of the dye solution the negatively charged sites on the membrane were competitively scrambled for by the positively charged methyl violet ions, hence, the decrease in q_e with time. Repulsion among the dye ions increased with time.

Effect of initial dye solution Ph

Scheme 1. Structure of methyl violet

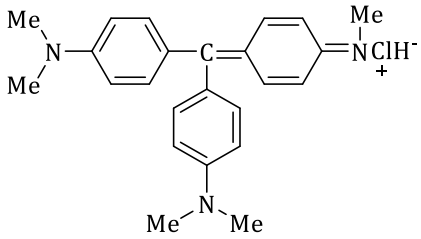

Table 1. Proximate analytical data of hen egg membrane

Parameter	Value (%)
Moisture	11.7
Ash	8.39
Crude protein	21
Carbohydrate	36.57
Fibre	27.59
Lipid	13.65

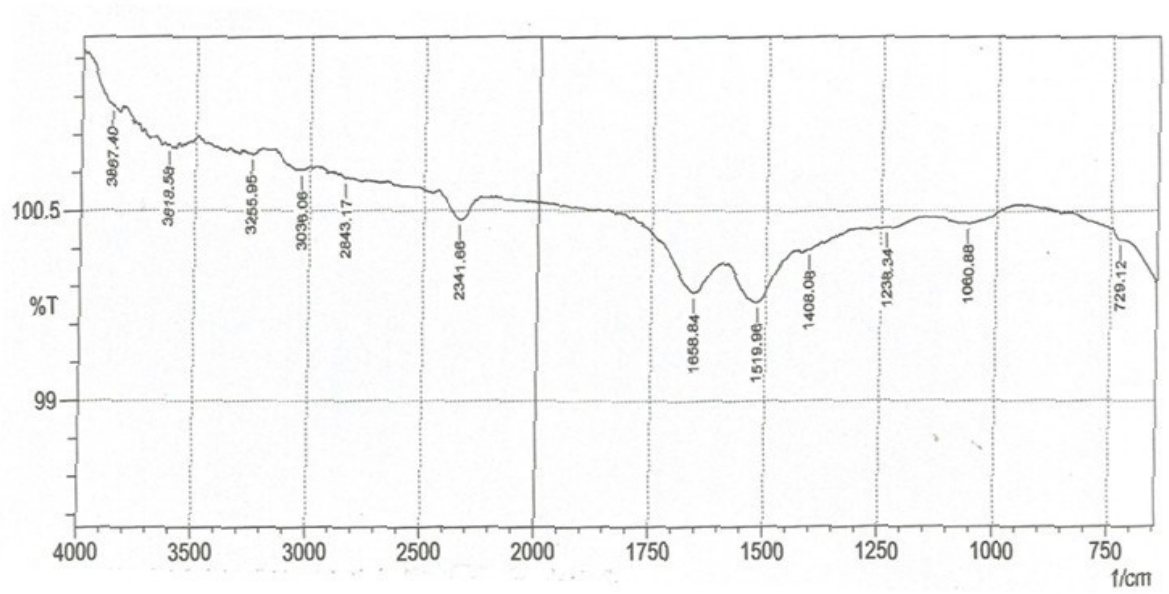

Figure 1. FT-IR spectrum of hen egg membrane

Dye solution pH is paramount in the biosorption of methyl violet on hen egg membrane in that it affects the properties of the biosorbent and the hen egg membrane [22]. Figure 4 shows the effect of initial solution pH on the biosorption of methyl violet on hen egg membrane. The pH range 6-10 was used. The highest q_e (56.25 mg/g) was obtained at pH 7 and 9. However, the q_e values at all the pH values used were close. The closeness in the values of q_e for all the used pH values used, for C_o 25 mg/L shows that the change in pH did not have great effect. This might be as a result of the zwitterionic nature of the protein fibre [23, 24].

Effect of biosorbent dosage

The effect of biosorbent dosage on the biosorption of methyl violet on hen egg membrane was investigated by contacting 25 mL portions of the dye with 0.01-0.16 g portions of the hen egg membrane at pH 8 and 30 °C. Figure 5 shows biosorbent dosage 0.01 g/25 mL having the highest q_e of 43.05 mg/g. After biosorbent dosage of 0.01 g/25 mL, the q_e decreased sharply. Increasing biosorbent dosage (0.01 to 0.16 g/25 mL) increased biosorption efficiency (67.28 to 95.44 %) while q_e decreased (42.05 to 3.728 mg/g). This phenomenon may be due to the occupation patterns of active sites at higher membrane doses. The unsaturated active sites of the membrane may be occupied as a result of particles aggregation and overlap which interferes with binding sites. This causes reduction in the total surface area of the membrane and q_e [12, 25, 26].

Effect of temperature

The effect of temperature on the biosorption of methyl violet on hen egg membrane was investigated by contacting 0.01 g portions of the membrane with 25 mL portions of dye solution of C_o 25–100 mg/L, pH 8 at 30, 45 and 60 °C. Figure 6 shows 30 °C having highest q_e of 13.494 mg/g for C_o 100 mg/L. The biosorption was for 180 min. For all the used C_o, q_e decreased with an increase in temperature. For each temperature, q_e increased with an increase in C_o. The decrease in q_e with increase in temperature was as a result of the weakening of the forces of attraction between the dye ions and the membrane surface. Increase in temperature (30 to 60 °C) led to a decrease (13.494 to 8.878 mg/g) in q_e. The result agrees with the work of *Horsfall Jnr* and *Spiff* (Table 5) [27].

Biosorption isotherm modeling

Adsorption isotherm is a relationship between the concentration of the adsorbate adsorbed onto the adsorbent and the adsorbate concentration in the solution at constant temperature [11]. An

adsorption isotherm is used to describe how adsorbate particles interact with the surface of the adsorbent. Equilibrium investigations are valuable in determining the adsorption capacity of the adsorbent and describe the adsorption isotherm by constants whose values give information on the surface properties and affinity of the adsorbents [28]. Methyl violet solution of C_o 25, 50 and 100 mg/L were biosorbed on egg membrane at 30 °C. Experimental data were analyzed with the Langmuir, Freundlich, Temkin, Redlich-Peterson and Sips models.

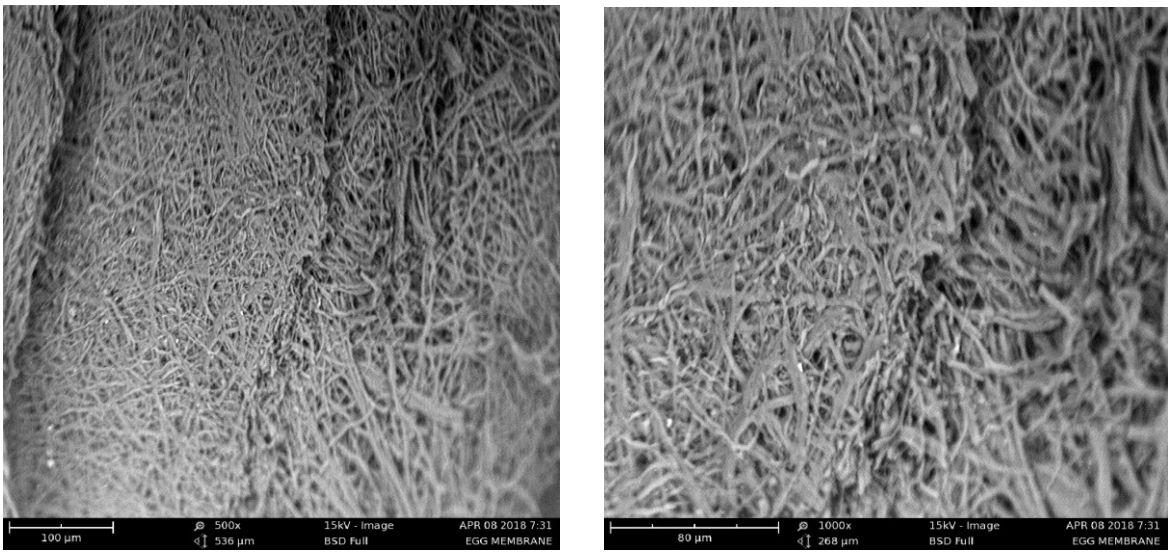

Figure 2. (a Scanning electron micrograph of egg membrane 500 xs, b). Scanning electron micrograph of egg membrane 1000x

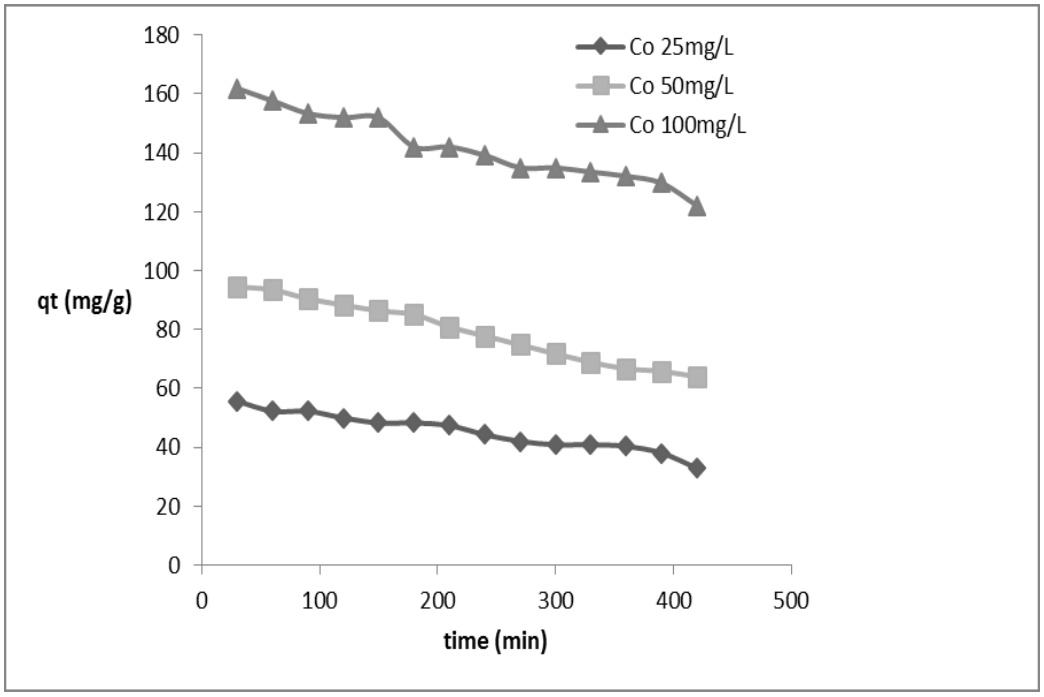

Figure 3. Biosorption of methyl violet on hen egg membrane at various C_o values at 30 °C

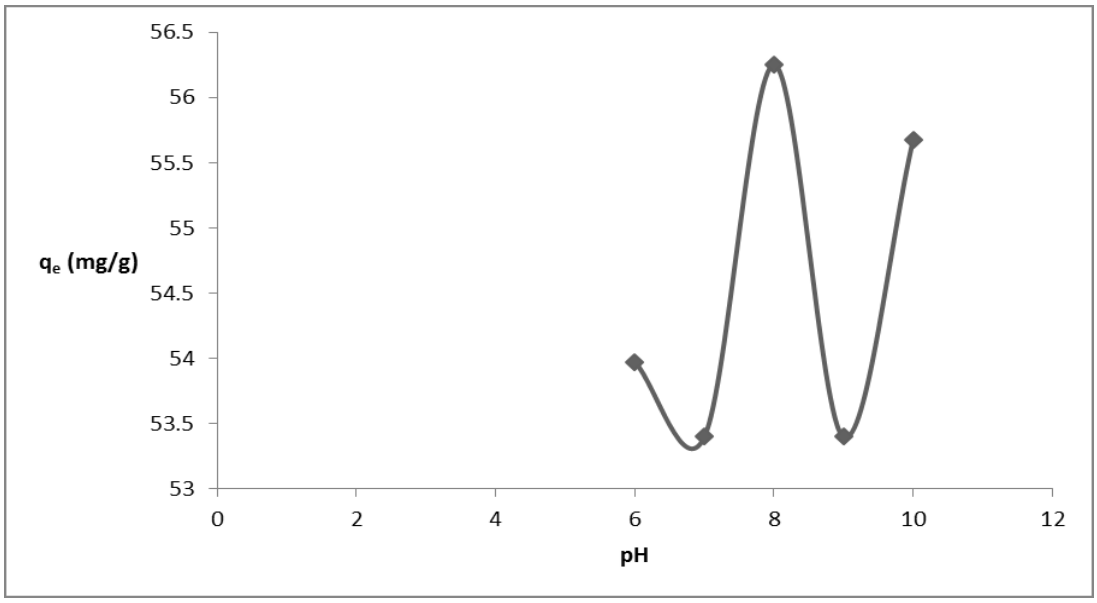

Figure 4. Biosorption of methyl violet on hen egg membrane at various pH values at 30 °C

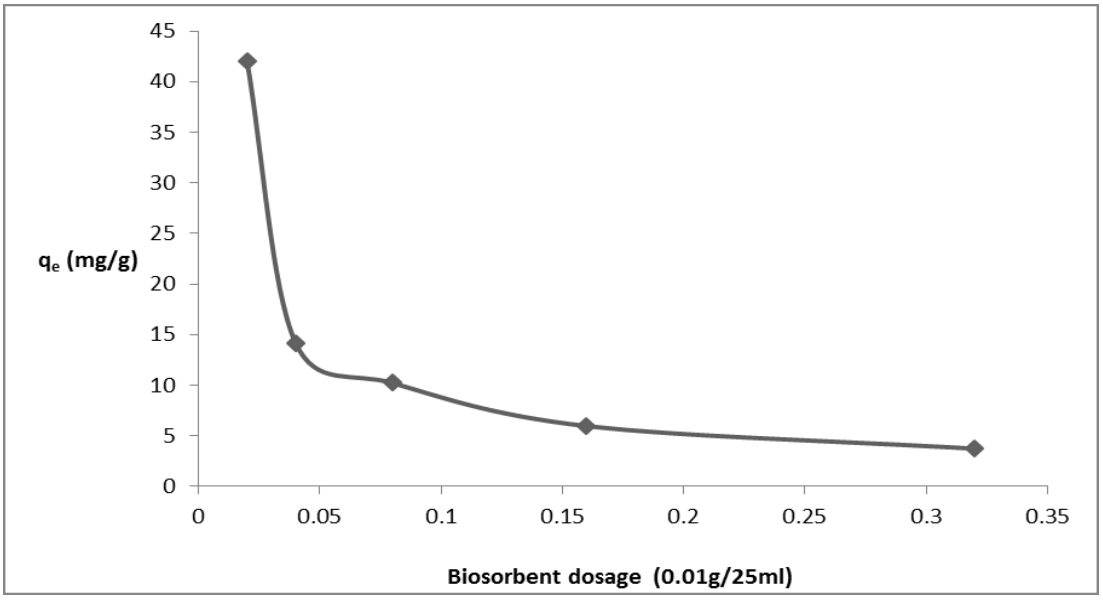

Figure 5. Biosorption of methyl violet on hen egg membrane at various biosorbent doses at 30 °C

Langmuir isotherm

The Langmuir isotherm [16] is based on a theoretical model under the assumption that there is monolayer adsorption over an energetically and structurally homogenous adsorbent surface. Saturation of the adsorbent is also accounted for. The Langmuir equation is expressed as Eq. 5:

$$q_e = \frac{q_o K_L C_e}{1 + K_L C_e} \quad 5$$

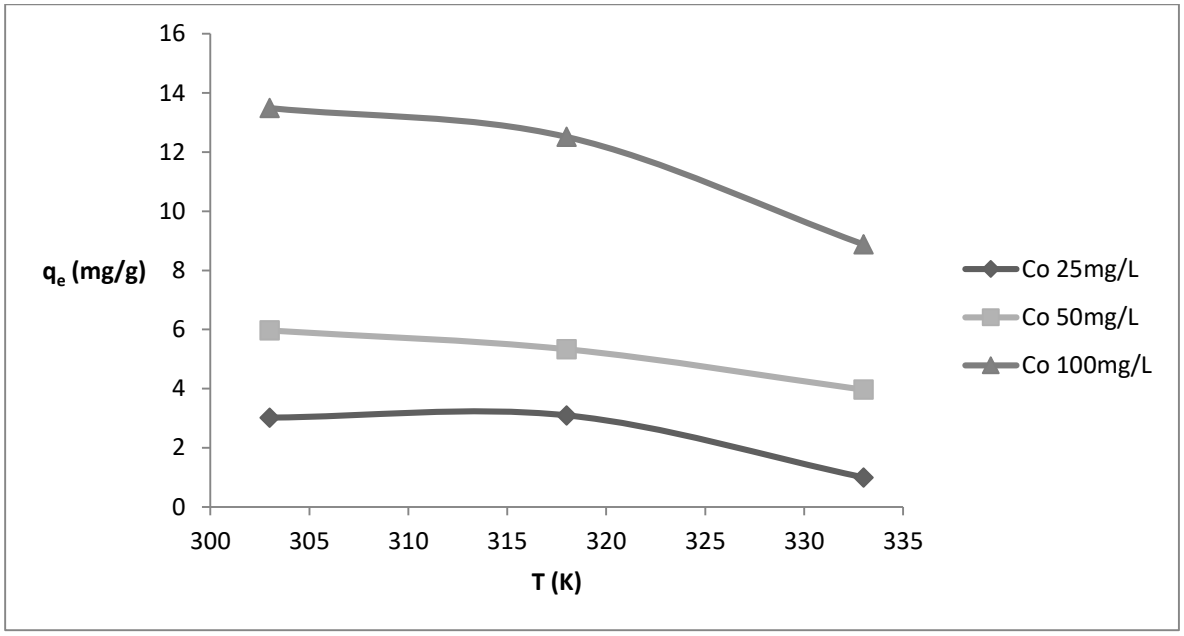

Figure 6. Biosorption of methyl violet on hen egg membrane at various temperature

The type 2 linearized form of Eq.5 is expressed as Eq.6:

$$\frac{1}{q_e} = \frac{1}{K_L q_m}\frac{1}{C_e} + \frac{1}{q_m} \quad 6$$

Where, q_m (mg/g) and K_L (L/mg) are the Langmuir constants related to the monolayer biosorption capacity and energy of biosorption respectively.

A plot of $^1/q_e$ vs $^1/C_e$ (Figure not shown) gave a straight line with slope $^1/K_L q_m$, and intercept $1/q_m$. The correlation co-efficient R^2, q_m and K_L values show that the Langmuir model was a good fit for simulating experimental data (Table 2). The Langmuir type 2 equation is used to explain equilibria phenomena of organic adsorption processes [29].

To prove that the biosorption was favorable, the dimensionless equilibrium parameter (R_L) was determined [30]. It is expressed as Eq.7:

$$R_L = \frac{1}{1 + K_L C_{om}} \quad 7$$

Where, C_{om} is the highest C_o.R_L<1, it shows that the process is favorable, R_L = 1, linear, R_L>1, unfavorable, and R_L = 0, irreversible.

Freundlich isotherm

This model is empirical and is used to describe systems that are heterogeneous. The Freundlich model assumes that the adsorption of the adsorbate takes place on a heterogeneous surface by multilayer adsorption and that the adsorbate concentration on the adsorbent infinitely increases with increase in adsorbate concentration [31, 32]. The Freundlich equation is expressed as Eq. 8:

$$q_e = K_F C_e^{1/n} \quad (8)$$

The linearized logarithmic form of the equation is expressed as Eq. 9:

$$Inq_e = (1/n)InC_e + InK_F \quad (9)$$

Where, K_F [mg/g (L/mg)$^{1/n}$] and n are Freundlich constants representing the biosorption capacity and biosorption intensity of the hen egg membrane respectively.

A plot of ln q_e vs ln C_e (Figure not shown) gave a straight line with slope $^1/n$ and intercept ln K_F values. Table 2 shows the $^1/n$ and K_F values. R^2 value (0.999) shows that this model was a very good fit for modeling the biosorption process.

The value of $^1/n$ ranges between 0 and 1; the surface heterogeneity increases as the $^1/n$ value gets closer to zero [33]. The n values show the extent of non-linearity between solution concentration and biosorption thus [34]: n = 1, adsorption is linear; n < 1, adsorption is chemisorption; n > 1, adsorption is physisorption.

The condition n > 1 is most common. This might be as a result of distribution of surface sites or any factor that brings about a decrease in adsorbent adsorbate interaction with increasing surface density [35]. The values of n within 1 to 10 portray good adsorption [36, 37]. In this work, the $^1/n$ and n values (0.9007 and 1.1102) show that the heterogeneity of the membrane surface was very low and the biosorption was a physisorption process.

Temkin isotherm

The Temkin model puts into consideration the effects of indirect adsorbate-adsorbate interactions on adsorption isotherm assuming that the heat of adsorption decreases linearly with adsorbent surface coverage due to sorbate-sorbate interactions [11]. It is expressed as Eq. 10:

$$q_e = \frac{RT}{b_T} In\ A_T C_e \quad (10)$$

Or as Eq. 11:

$$q_e = \frac{RT}{b_T} InA_T + \frac{RT}{b_T} In\ C_e \quad (11)$$

Where, A_T (L/g) is Temkin constant corresponding to the maximum binding energy, b_T (J/mol) the Temkin constant related to heat of adsorption, R, (8.314 J/mol. K) gas constant and T(K) the absolute temperature.

A plot of q_e vs ln C_e gave a straight line with slope RT/b_T and intercept $(RT/b_T)\ ln\ A_T$ (Figure not shown). Table 2 shows the R^2, A_T and b_T values. The R^2 value (0.9693) makes the Temkin model a good fit for simulating the biosorption of the dye on the membrane.

Redlich–Peterson isotherm

The Redlich-Peterson model is a three parameter isotherm model [38]. It approaches the Freundlich model at high concentrations, and agrees with the Langmuir model at low adsorbate concentrations. The Redlich-Peterson equation is expressed as Eq. 12:

$$q_e = \frac{K_{RP} C_e}{1 + d_{RP} C_e^{\beta}} \quad (12)$$

Eq. 12 can be linearized as Eq. 13:

$$\frac{C_e}{q_e} = \frac{a_{RP} C_e^{\beta}}{K_{RP}} + \frac{1}{K_{RP}} \quad (13)$$

Where, K_{RP}, α_{RP} and β are the Redlich-Peterson parameters. β lies between 0 and 1.
The logarithmic form of Eq. 13 gives Eq. 14:

$$ln\left(C_e/q_e\right) = ln\left(a_{RP}/K_{RP}^2\right) + \beta ln C_e \quad (14)$$

A plot of $ln\ (C_e/q_e)$ vs $ln\ C_e$ gave a slope equal to β, intercept $ln\ (\alpha_{RP}/K^2_{RP})$ and R^2 0.9944 (Figure not shown). Substituting the value of β (0.1051) in Eq.13 and plotting C_e/q_e vs C_e^{β} gave a straight line (Figure not shown) with slope equal to α_{RP}/ K_{RP} and intercept $^1/ K_{RP}$. The R^2 value (0.9945) shows that this model is a good fit for analyzing experimental data. Table 2 shows the α_{RPc} and K_{RP} values.

Sips isotherm model

Sips isotherm model is a combination of Langmuir and Freundlich isotherm models. It describes heterogeneous surfaces far better. It reduces to Freundlich isotherm at low adsorbate concentrations and to Langmuir isotherm at high adsorbate concentrations [12, 38, 39]. It is expressed as Eq. 15:

$$q_e = \frac{q_m(K_s C_e)^{\gamma}}{1(K_S C_E)^{\gamma}} \quad 15$$

Rearrangement and expansion of Eq. 15 gives Eq. 16:

$$q_e = q_m K_s^{\gamma} C_e^{\gamma} + q_m \quad 16$$

The logarithmic form of Eq. 16 is Eq. 17:

$$lnq_e = l\,n\left(q_m^2 K_s^{\gamma}\right) + \gamma lnC_e \quad 17$$

A plot of lnq_e vs lnC_e gave a straight line with slope equal to γ (Figure not shown). Substituting γ (1.1183) in Eq.16 and plotting q_e vs C_e^{γ} gave a straight line with slope equal to $q_m K_s^{\gamma}$ and intercept equal to q_m (Figure not shown). Table 2 shows the K_S, q_m and γ values. R^2 value (0.9978) shows that the Sips model is a good fit for modeling the biosorption of methyl violet on hen egg membrane.

All the applied isotherm models applied favored the biosorption process as shown in Figure 7. This is explained by the fact that all the q_e vs C_e curves are convex [40].

Adsorption kinetic modeling

Prediction of adsorption rate would help in designing batch adsorption systems [11]. In this work, the pseudo-second order (PSO), Elovich and Boyd models were applied to determine the kinetics, mechanism and rate controlling step of the biosorption.

Pseudo-second order kinetic model

The PSO kinetic model [9] is expressed as Eq. 18:

$$t/q_t = 1/(K_2 q_o^2) + t/q_o \quad 18$$

Where, k_2 [g/mg min] is the rate constant. A plot of t/q_t versus t (Figure not shown) gave a straight line with slope and intercept equal to $1/q_o$ and $1/(k_2 q_o^2)$ respectively.

The initial biosorption rate h (mg/g min) is expressed as Eq. 19:

$$h = k_2 q_o^2 \quad (19)$$

Table 3 shows the values of q_o and k_2 for C_o 25, 50 and 150 mg/L. R^2 values 0.9718, 0.9886 and 0.9945 for C_o 25, 50 and 100 mg/L respectively show that PSO model analyzed the experimental data suitably.

Elovich kinetic model

Elovich kinetic model equation [11] is expressed as Eq. 20:

$$q_t = \left(1/b\right) ln(ab) + \left(1/b\right) ln\, t \quad (20)$$

Where, a (mg/g min) is the initial biosorption rate and b (g/mg) is the desorption constant related to the extent of surface coverage and activation energy for chemisorption.

A plot of q_t against *ln* t gave a straight line with slope equal to 1/b and intercept equal to (1/b) *ln(ab)* (Figure not shown).

Table 3 shows the values of a and b for C_o 25, 50 and 100 mg/L. R^2 values 0.842, 0.8595 and 0.8991 for C_o 25, 50 and 100 mg/L respectively show that this model is a good fit for experimental data.

Boyd kinetic model

Table 2. Isotherm parameters for biosorption of methyl violet on hen egg membrane at 30 °C

Model	Parameters	Values
Langmuir	K_L (L/mg)	0.0051
	q_m (mg/g)	588.24
	R_L	0.662
	R^2	0.9979
Freundlich	$^1/n$	0.9007
	n	1.1102
	K_F [mg/g (L/mg)$^{1/n}$]	3.554
	R^2	0.9999
Redlich-Peterson	A_T (L/g)	7.426
	b_T (J/mol)	41.25
	R^2	0.9693
	α_{RP}	95.931

	K_{RP}	344.828
	β	0.1051
	R^2	0.9945
	K_s	0.129
Sips	q_m (mg/g)	13.293
	γ	1.1183
	R^2	0.9978

Table 3. Kinetic models parameters for the biosorption of methyl violet on hen egg membrane

Model		Values		
		C_o (mg/L)		
		25	50	100
PSO	K_2 (g/mg.min) x10^{-4}	7.98	4.842	4.126
	h (mg/g min)	0.962	1.868	6.289
	q_o (mg/g)	34.72	62.11	123.457
	R^2	0.9718	0.9886	0.9945
	RMSE	1.77	1.89	1.33
Elovich	a (mg/g.min)	0.169	0.371	0.454
	b (g/mg)	20.04	11.792	10.881
	R^2	0.842	0.8595	0.8991
Boyd	B	0.1147	0.3071	0.2655
	R^2	0.9449	0.9186	0.9526
Sticking probability	E_a	11.895	22.359	15.458
	S*	0.0022	0.0007	0.0016
	R^2	0.5111	0.94	0.968

Table 4. Thermodynamic parameters for the biosorption of methyi violet on hen egg membrane

C_o (mg/L)	Parameter/Value							
	ΔH^o	ΔS^o	ΔG^o_{ads}			K_D		
			30°C	45°C	60°C	30°C	45°C	60°C
25	60.966	190.199	-3.084	-0.367	2.703	3.401	3.241	6.331
50	29.194	85.95	-3.109	-2.03	-0.129	1.157	2.155	4.028
100	40.261	116.554	-5.11	-2.03	-0.76	0.342	1.05	1.316

There are two mechanisms encountered in adsorption, the intraparticle diffusion and liquid film diffusion [22–41]. The mechanism that controls this process is ascertained by the Boyd model expressed as Eq. 21:

$$F = 1 - \frac{6}{\pi^2}\sum_{n=1}^{\infty}\frac{1}{n^2}\exp(-n^2 B_t) \quad 21$$

Where, B_t is a mathematical function of F. F is the ratio of q_t and q_e expressed as Eq. 22:

$$F = {}^{q_t}/_{q_e} \quad 22$$

Where, $q_t < q_e$ or

$$F = {}^{q_e}/_{q_t} \quad 23$$

Where, $q_t > q_e$.

Transformation and approximation of Eq. 21 gives Eqs. 24 and 25:

$$B_t = -0.4977 - ln(1 - F)\ for\ F = 0.86 - 1.0 \quad 24$$

$$B_t = \left[\sqrt{\pi} - \sqrt{\pi - \left(\frac{\pi^2 F}{3}\right)}\right]^2 for\ F = 0 - 0.85 \quad 25$$

A plot of B_t against t gave a straight line (Figure not shown) with slope B, termed the Boyd constant. If the straight line passes through the origin, intraparticle or pore diffusion will be the rate limiting step. If the straight line does not pass through the origin, liquid film diffusion will be the rate limiting step [42]. None of the straight lines obtained from the plots passed through the origin, showing that the process was controlled by liquid film diffusion. Table 3 shows the values of B and R^2 for C_o 25, 50 and 100 mg/L. The R^2 values which are generally above 0.9 show the lines to be straight.

Sticking Probability

The mechanism in an adsorption process can also be measured by using the modified Arrhenius type equation which is related to surface coverage (θ) [27]. The relation is expressed as Eq. 26:

$$S^* = (1-\theta)exp - \left({}^{E_a}/_{RT}\right) \quad 26$$

Where, S* is the sticking probability and E_a the activation energy. The logarithmic form of Eq. 26 is expressed as Eq. 27:

$$ln(1-\theta) = lnS^* + {}^{E_a}/_{RT} \quad 27$$

A plot of ln (1–θ) against 1/T gave a straight line with slope equal to E_a/R and intercept *ln*S* (Figure not shown). S* indicates the measure of the potential of an adsorbate to remain on the adsorbent indefinitely.

- If S* >1, there is no adsorption
- if S* = 1, there is a possible mixture of physisorption and chemisorption
- if S* = 0, indefinite chemisorption predominates
- 0<S*<1, there is a favorable sticking of adsorbate to adsorbent. Physisorption predominates

Table 3 shows the E_a, S* and R^2 values for C_o 25, 50 and 100 mg/L. The R^2 values show the model fit for experimental data while the E_a and S* values show physisorption, since E_a is low and S* less than 1.

Biosorption thermodynamics

The biosorption process can be evaluated by applying the thermodynamic parameters: standard enthalpy (ΔH^o), entropy (ΔS^o) and free energy (ΔG^o). These parameters are expressed as Eqs. 28, 29 and 30:

$$lnK_D = \frac{\Delta S^o}{R} - \frac{\Delta H^o}{RT} \quad 28$$

Where, K_D is the distribution (or adsorption equilibrium) constant [11] expressed as Eq. 29:

$$K_D = \frac{(C_o - C_e)e}{C_e} \quad 29$$

$$\Delta G^O = -RTlnK_D \quad 30$$

A plot of ln K_D against 1/T (Figure not shown) gave a straight line with slope equal to ΔH^o /R and the intercept equal to ΔS^o/R. R^2 values (>0.8) shows that the lines are straight. Table 4 shows the K_D, ΔH^o, ΔS^o and ΔG^o values for C_o 25, 50 and 100 mg/L respectively.

The ΔG^o values are negative and their magnitudes less than 20 kJ/mol. Hence, the process was spontaneous and physisorptive [43, 44]. The positive values of ΔH^o show that the biosorption was exothermic while the positive values of ΔS^o suggest increasing randomness at the biosorbent-biosorbate interface and affinity for the biosorbent [45, 46].

Table 5. Maximum experimental biosorption capacity of hen egg membrane and other biosorbents

Biosorbent	Dye	%Removal	References
Hen egg membrane	methyl violet	48.86	This work
Hen egg membrane	2,4-DCP	48.2,71.2	*Koumanova* et al. [46]
	3,5-DCP	37.2, 74.4	*Koumanova* et al. [46]
Hen eggshell	methylene blue	84-73	*Hassan* and *Salih* [12]

Conclusion

Biosorption of methyl violet on egg membrane in a batch process was carried out at various C_o (25, 50 and 100 mg/L), pH (6-10), biosorbent dosages (0.01, 0.02, 0.04, 0.08 and 0.16 g/25 mL) and temperatures (30, 45 and 60 °C). Experimental data were analyzed with Langmuir, Freundlich, Temkin, Redlich–Peterson and Sips isotherm models as well as PSO and Elovich kinetic models. Results show that the highest biosorption capacity was obtained from C_o 100 mg/L, pH 8, biosorbent dosage 0.01 g/25 mL and temperature 45 °C. Biosorption capacity increased with an increase in C_o

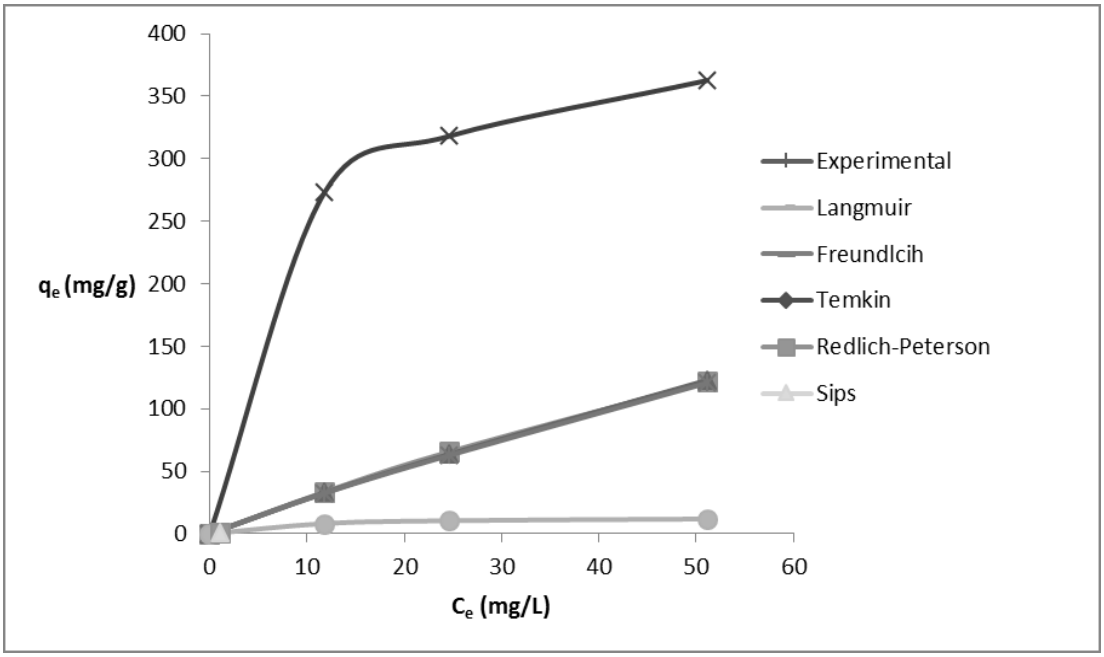

Figure 7. Isotherm curves for batch biosorption of methyl violet on hen egg membrane

but decreased with an increase in time. The five isotherm models applied, analyzed experimental data, suitably (R^2>0.95). R^2 values for PSO and Elovich kinetic models (>0.84) show that the models were good fits for experimental data. Application of Boyd kinetic model shows that the biosorption was controlled by liquid film diffusion. Sticking probability S*, E_a, ΔG_{ads}, ΔH and ΔS values for 25, 50 and 100 mg/L initial dye concentrations show that the biosorption was physisorptive, spontaneous and endothermic. There was an increased randomness at the solid-solution interface and high affinity of the dye ions for the hen egg membrane. The results show that egg membrane is a good biosorbent for methyl violet, a cationic dye.

Disclosure statement

No potential conflict of interest was reported by the authors.

Orcid

Beniah O. Isiuku 0000-0002-5681-7170

References

[1]. Isiuku B.O., Nwosu C.N. Asian *J. Chem.*, 2017, **29**:475

[2]. Isiuku B.O., Horsfall M., Spiff A.I. *Res. J. Appl. Sci.*, 2014, **9**:201

[3]. Belay K., Hayelom A. *Chem. Mater. Res.*, 2014, **6**:31

[4]. Pal J., Deb M.K., Deshmukh D.K., Sen B.K. *Appl. Nanoscience*, 2014, **4**:61

[5]. Saji M., Taguchi S., Uchiyama K., Osono E., Hayama N., Ohkuni H. *J. Hosp. Infect.*, 1995, **31**:225

[6]. Li P., Su Y.J., Wang Y., Liu B., Sun L.M. *J. Hazard. Mater.*, 2010, **179**:43

[7]. Bonetto L.R., Ferrarini F., de Macro C., Crespo J.S., Guegan R., Giovanela M. *J. Water Proces. Eng.*, 2015, **6**:11

[8]. Turhan K., Durukan I., Ozturkcan S.A., Turgut Z. *Dyes. Pigments*, 2012, **92**:897

[9]. Tong Z., Zheng P., Bai B. *Catalysts*, 2016, **6:**58

[10]. Wang L., Zhang J., Zhao R., Li C., Zhang C. *Desalination*, 2010, **254**:68

[11]. Njoku V.O., Ayuk A.A., Oguzie E.E., Ejike E.N. *Sep. Sci. Technol.*, 2012, **47**:753

[12]. Hassan A.A., Hassan, Z.A.S. *Euphrates J. Agric. Sci.*, 2013, **5**:11

[13]. Pramanpol N., Nitayapat N. *Kasetsart J. Nat. Sci.,* 2006, **40**:192

[14]. Association of Official Analytical Chemists (AOAC), *Official Methods of Analysis*, 15th Ed., Arlington, VA, USA, 1990, p. 331

[15]. Akinola L.K., Umar A.M. *J. Appl. Sci. Environ. Manage.*, 2015, **19**:279

[16]. Rocha P.D., Franca A.S., Oliveira L.S. *Int. J. Eng. Technol.*, 2015, **7**:459

[17]. Williams D.H., Fleming I. *Spectroscopic Methods in Organic Chemistry*, 3rd Ed., McGraw-Hill Book (UK) Ltd., 1980, pp. 49

[18]. Finar I.L. *Organic Chemistry*, Vol. 2, 5th Ed., Longman Group Ltd, Essex, UK, 1975, pp.651

[19]. Han R., Zou W., Yu W., Cheng S., Wang Y., Shi J. *J.Hazard. Mater.*, 2007, **141**:156

[20] Tsai W.T., Yang J.M., Lai C.W., Cheng Y.H., Lin C.C., Yeh C.W. *Bioresource Technol.*, 2006, **97**:488

[21]. Njoku V.O., Hameed B.H. *Chem. Eng. J.*, 2011, **173**:391

[22]. Finar I.L., *Organic Chemistry*, Vol. 1: The Fundamental Principles, 6th Ed., Longman Group Ltd, London, 1973, p. 207

[23]. Jones Jr M., *Organic Chemistry*, 2nd Ed., W.W. Norton and Company Inc., 2000, p. 715

[24]. Yeddou N., Bensmaili A. *Desalination*, 2007, **206**:127

[25]. Mezenner N.Y., Bensmaili A. *Chem. Eng. J.*, 2009, **147**:87

[26]. Horsfall Jnr M., Spiff A.I. *Electron. J. Biotechnol.*, 2005, **8**:162

[27]. Sen J.K. *Int. J. Environ. Pollut.*, 2011, **3**:1

[28]. Isiuku B.O., Onyema M.O., *World News Nat. Sci.*, 2017, **13**:10

[29]. Bello O.S., Fatona T.A., Falaye F.S., Osulale O.M., Njoku V.O. *Environ. Eng. Sci.*, 2010, **29**:186

[30]. Shrivastava P.K., Gupta S.K. *Int. J. Chem. Sci. Appl.*, 2015, **6**:1

[31]. Rane N.M., Sapkal R.S., Sapkal V.S., Patil M.B., Shewale S.P. *Int. J. Chem. Sci. Appl.*, 2010, **1**:65

[32]. Ajmal M., Khan A.H., Ahmad S., Ahmad A. *Water Res.*, 1998, **32**:3085

[33]. Al-Fatlawi A.H., Neamah M.M. *Int. J. Adv. Res. Sci. Eng. Technol.*, 2015, **2**:557

[34]. Reed B.E., Matsumoto M.R. *Separat. Sci. Technol.*, 1993, **28**:2179

[35]. Mckay G., Otterburn M.S., Sweeney A.G. *Water Res.*, 1980, **14**:15

[36]. Ozer A., Pirinc H.B. *J. Hazar. Mater.*, 2006, **137**:849

[37]. Oubagarandin J.U.K., Murthy Z.V.P., Rao P.S. *Ind. Chem. Eng.*, 2007,**49**:196

[38]. Shahruyari Z., Goharrizi A.S., Azadi M. *Int. J. Water Resour. Environ. Eng.*, 2010, **2**:016

[39]. Vasailis I.J. *J. Eng. Studies Res.*, 2010,**16**:29

[40]. Ekpete O.A., Horsfall Jnr. M., Spiff A.I. *J. Nat. Appl. Sci.*, 2012, **1**:106

[41]. Reichenberg D. *J. Amer. Chem. Soc.*, 1853,**78:**589

[42]. Ding L., Zou B., Gao W., Liu Q., Wang Z., Guo Y., Wang X., Liu Y. *Colloids Surf. A*, 2014, **446**:1

[43]. Konicki W., Cendrowski K., Chen X., Mijowska E. *Chem. Eng. J.*, 2013, **228:**824

[44]. Rachamani J., Mousavi H.Z., Behzad M. *Desalination*, 2011, **267**:256

[45]. Li C., Dong Y., Yang J., Li Y., Huang C. *J. Mol. Liq.*, 2014, **196**:348

[46]. Koumanova B., Peeva P., Allen S.J., Gallagher K.A., Healy M.G. *J. Chem. Technol. Biotechnol.*, 2002, **77:**539

How to cite this manuscript: Beniah O. Isiuku*, Chigoziri Ugwueze Nwogu. Cationic dye (methyl violet) removal from aqueous solution by egg membrane in a batch biosorption process. *Asian Journal of Green Chemistry*, 3(2) 2019, 236-257. DOI: 10.33945/SAMI/AJGC.2019.3.8